Volume 9, Issue 2, 2020, 1089 - 1098 **ISSN 2284-6808**

Letters in Applied NanoBioScience

https://nanobioletters.com/

https://doi.org/10.33263/LIANBS92.10891098

Original Research Article **Open Access Journal**

Received: 02.05.2020 / Revised: 14.05.2020 / Accepted: 15.05.2020 / Published on-line: 18.05.2020

Layer by layer deposited osteoinductive scaffolds for bone tissue engineering

Shivaji Kashte [1], Sachin Kochrekar [2,3], Rakesh Kumar Sharma [4], Sachin Kadam [1, 5]

[1] Department of Stem Cell & Regenerative Medicine, Centre for Interdisciplinary Research, D. Y. Patil Education Society (Institution Deemed to be University), Kolhapur 416006, India

[2] Organic Synthesis Laboratory, Department of Applied Chemistry, Defense Institute of Advanced Technology(DU), Pune-411025, India

[3] Turku University Centre for Materials and Surfaces (MATSURF), Laboratory of Materials Chemistry and Chemical Analysis, University of Turku, FIN-20014, Turku, Finland

[4] D.Y. Patil Medical College, D. Y. Patil Education Society (Institution Deemed to be University), Kolhapur 416006, India

[5] Advancells Group, NOIDA, Uttar Pradesh 201301, India

*corresponding author e-mail address: ***kadamsachin@gmail.com*** | Scopus ID 57208832048

ABSTRACT

There are various bone regenerative and repair methods, but the use of osteoinductive scaffolds as bone grafts/substitute has gained wide importance worldwide. Here, an osteoinductive scaffold is developed which spontaneously stimulates stem cells to osteoblast formation without the use of any growth factor or differentiation media. We prepared electrospun PCL scaffold which is further modified for osteoinductivity by layer-by-layer method using graphene and *Cissus quadrangularis* callus culture extract (PCL-GP-CQ). The modified PCL-GP-CQ scaffold was compared with plain PCL scaffold and PCL coated only with GP. Physical properties such as roughness, wettability, yield strength and tensile strength of PCL-GP-CQ scaffold were found to be superior. Also, PCL-GP-CQ scaffold when seeded with human umbilical cord Wharton's jelly derived mesenchymal stem cells showed higher *in vitro* biocompatibility with enhanced cellular proliferation on its surface. Synergistic effect of graphene and *Cissus Quadrangularis* callus culture extract in scaffold boosted the differentiation of human Umbilical Cord Wharton's jelly derived Mesenchymal Stem Cells into osteogenic lineage without any differentiation media in less than 20 days. The PCL-GP-CQ scaffold enhanced osteoblastic differentiation, osteoconduction and osteoinduction potential of scaffolds making them highly suitable for bone regeneration and bone tissue engineering applications.

Keywords: *Scaffolds; graphene; Cissus quadrangularis; Human umbilical cord Wharton's jelly-derived Mesenchymal stem cells; Bone tissue engineering.*

1. INTRODUCTION

Bone defects and repair are the most common problems encountered worldwide [1]. Bone is the second most transplanted tissue after blood [2]. As a matter of fact, the development and progress of bone tissue engineering have focused on using artificial materials for the regeneration, repair, or restructuring of bone tissues [2]. The various polymers like poly ε-caprolactone (PCL), poly-d, l-lactic acid (PDLLA) [3], poly (L/DL-lactide) (PLDL) [4], PLLA [5], poly (DL-lactic-co-glycolic acid) (PLGA) [6] have shown to be potent in terms of their mechanical properties like tensile strength, elastic modulus, biocompatibility, higher cellular properties and even bone formation *in vivo* [2]. Among these, PCL is extensively used FDA approved biocompatible and biodegradable material with varied tissue engineering applications. PCL along with Hydroxyapatite (HA) [7], PCL-gelatin hybrid nanofibrous membranes [8], PCL-(Poly-1,4- butylene adipate-co-polycaprolactam--HA scaffold [9], are used in bone tissue engineering.

However, for tissue engineering application hydrophobic PCL is required to modify to partly hydrophilic nature by different surface modification methods [10]. Surface modification is one of the crucial factors, identified to be responsible for cellular attachment and enhanced cellular proliferation. Surface modification also helps in the improvement of the biological properties of scaffolds. This interaction between tissue and foreign surface largely depends upon surface properties of materials such as wettability, roughness or topography, surface charge, and chemistry [11,12].

A layer-by-layer method is a simple, relatively fast, environmentally benign, and economic process [13] that prepares uniform multilayer films on substrates. The deposition is fast and irreversible, with controlled deposition thickness and uniform surface coverage [14]. Layer-by-layer deposition significantly improves wettability and mechanical strength of scaffold [13]. The transformation of the hydrophobic electrospun block copolymer to the hydrophilic mesh using layer-by-layer method has shown significant improvement in cell viability and cell attachment [10,15,14].

Graphene (GP) is the emerging material today. Graphene (2D structure) is the only form of carbon in which every single atom is in exposure for a chemical reaction from either side [16]. The interaction GP with stem cells revealed cellular compatibility and ability to support differentiation of stem cells into osteoblasts, chondroblasts and neuronal lineages [17–19]. The ancient Ayurveda book 'Bhawa Prakash Samita' described the medicinal properties of *Cissus quadrangularis* (CQ). Along with antimicrobial and antioxidant activity[20], methanolic extract of CQ has proven to be useful for bone fracture healing [21,22] due to its high calcium ions (4% weight) and phosphorous content. It is believed that active constituents of CQ promote proliferation and differentiation of MSCs into osteoblasts that helps in bone formation [23]. CQ callus extract accelerates fracture healing and early remodelling of fracture. A phytogenic isolated steroid may be the main constituent in CQ. It has been observed that CQ acts by stimulation of metabolism with an increased expression of

osteopoietin and increased uptake of minerals such as calcium, sulphur, and strontium by osteoblasts in fracture healing [24].

In the following study, porous PCL electrospun scaffolds were modified with GP and CQ using layer-by-layer method. These composite scaffolds help to demonstrate morphological, physical and biological characteristics that are suitable for bone tissue.

2. MATERIALS AND METHODS

2.1. Materials.

Chemicals were procured from Sigma Aldrich (USA) and cell culture growth media and supplements from Invitrogen (CA, USA) unless specified.

2.2. *Cissus quadrangularis* callus culture and preparation of callus culture extract.

Cissus quadrangularis (CQ) callus culture and its extract was prepared as reported earlier in our studies [25,26]. In brief, CQ plant was identified and collected from Kolhapur region of Maharashtra, India. The callus of CQ was obtained by using MS medium No.6 (Hi-Media, India) (2.26 g/L) along with NAA (α-Naphthalene acetic acid), 2.5 mg/L(Hi-Media, India), BAP (6-Benzylaminopurine), 0.5 mg/L (Hi-Media, India), sucrose 40 g/L (Hi-Media, India), Agar (10 g/L) (Hi-Media, India). The 70% ethanol (v/v) and 0.01% $HgCl_2$ (mercuric chloride) solution used for surface sterilization of CQ stems. These surface-sterilized explants were inoculated into MS media and culture tubes were incubated in dark at room temperature 28ºC. These culture tubes were observed daily for callus formation for 3-4 weeks.

Fully-grown callus from 4-5 weeks grown culture was selectively dehydrated, dried and a fine powder was made. The crude extract was prepared by using a Soxhlet apparatus with ethanol and was partitioned using petroleum ether. This extract was checked for the presence of phytosterol using Salkowski test [27]. Briefly, the extract was dissolved in chloroform and few drops of concentrated sulphuric acid were added. The presence of of phytosterol was confirmed by visualization of a brown ring at the bottom of the test tube. . This pure form of CQ extract was used for further surface medication of scaffolds.

2.3. Preparation of scaffolds by electrospinning.

Poly ε-caprolactone (PCL) solution (10% w/v) was used for scaffolds preparation. Solvents used were Tetrahydrofluran (THF): Methanol (3:1) and 30 h of magnetic stirring. PCL scaffolds were fabricated by electrospinning with a flow rate of 0.8 mL/h and a voltage of 12kv. The distance between the tip of syringe and collector was adjusted to 12.5 cm. PCL scaffolds were then used for further surface modifications.

2.4. Modification of scaffolds using layer by layer method.

Few layer graphene sheets (GP) (particle Size of 100 to1000 nm) were prepared by a method described by Ruoff *et al* [28]. The solutions of GP (1 mg/mL) and CQ (1 mg/mL) were prepared separately, by dispersing components in distilled water through sonication. These solutions were used to modify the surface of electrospun PCL scaffolds. PCL- GP scaffold was prepared by simply dipping PCL scaffold repetitively in GP solution for 2 min followed by air drying. Similarly, PCL-GP-CQ scaffold was prepared by dipping PCL scaffold first in GP solution and then in CQ solution, alternatively for 2 min with intermittent air-drying cycles. 30-, 60-, and overnight coating cycles were used for surface modification to determine the most effective surface coating.

The leaching of the additives (GP) from the scaffolds was investigated as per ISO-10993-12. The leaching was least in the 60 cycles followed by overnight dipped samples and then 30 cycles of the coating. This could be due to more interaction between PCL and GP in the 60 dipped cycles of coating. In the overnight dipped samples, the deposition was not uniform. Therefore, we chose 60 cycles over 30 cycles and overnight dipped samples because of more uniform deposition as well as less leaching. The leaching study was not significant as there was a very small amount of GP in the leached solution. (supporting information).

2.5. Characterization of Scaffolds.

The prepared scaffolds were characterized for morphological, physical, mechanical and biological properties.

Morphological analysis.

The fiber diameter of electrospun PCL and surface modified scaffolds was examined by field emission scanning electron microscope (FESEM, Carl Zeiss, Germany) at an accelerating voltage of 15 kV. In case of FESEM, scaffolds were cut into 5x5 mm squares, mounted on to sample stubs and sputter-coated with gold using SC 7640 sputter coater (Quorum Technologies Ltd, UK). The coated GP was then analysed on electrospun fibers of PCL. From FESEM micrographs, scaffold fiber diameter was measured using image analysis software (ImageJ, National Institutes of Health, Bethesda, USA).

Surface morphology of PCL and surface modified scaffolds was analysed by atomic force microscopy (AFM, Asylum Research) using tapping mode. The scaffolds were cut into small pieces and were stuck on a glass slide using cellophane tape. Scan rate of 1.0 Hz and scan area of 10μm was used for imaging.

Physical analysis.

Fourier Transform Infra-Red (FTIR) spectra were recorded for all scaffolds (FTIR Brucker, Germany). The spectra were obtained with 30 scans per sample ranging from 3000 to 500 cm^{-1}.

Wetting properties.

The water contact angle was analyzed by the sessile drop method using drop shape image analysis software. A droplet of pure water was deposited vertically on to the surface and contact angles were measured by contact angle goniometer (KRUSS, Germany) using an optical subsystem. The angle formed between the solid/liquid interface and the liquid/gas interface was determined as the liquid contact angle. Contact angle measurement of liquid droplets on a solid substrate (n=3) was used to measure surface wettability of the scaffolds.

Mechanical Properties.

Tensile properties were calculated at room temperature using a universal tensile machine (STS 248, Star Testing Systems, India). The scaffold was cut into cylinders (n=3) and tested. The maximum loading capacity was 100 N with a strain rate of 5mm/min. Accordingly, the resulting stress-strain curves, yield strength and tensile strength were calculated [27,29,30].

2.6. Isolation and Culture of hUCMSCs.

Isolation and culture of human Umbilical Cord Wharton's Jelly derived mesenchymal stem cells (hUCMSCs) was performed as mentioned in our previous studies [25,26,31]. Human umbilical

cords were collected from caesarean deliveries with patient consent. In sterile condition, blood and blood clots were removed from collected cords with PBS.. 10% betadine solution was used for cord surface disinfection. Then cord was chopped into 1-2 mm pieces and cord tissue was treated with Collagenase Type IV: Dispase II (7:1v/v) for 30 min and later in Trypsin (0.05%)-EDTA (0.02%) for a further 20 min at 400 rpm and 37ºC on a magnetic orbital shaker. The homogenate was then filtered through a sterile muslin cloth and centrifuged at 1500 rpm for 10 min. The obtained cell pellet was cultured in Dulbecco's Modified Eagle's Medium (DMEM): Ham's F12 (DMEM: HF12, 1:1) medium complemented with 10% foetal calf serum, penicillin (100 units/mL) and streptomycin (100 µg/mL). The cells were incubated for 48 h at 37ºC, 5% CO_2 and passaged after every 48 h. The isolated hUCMSCs were cryopreserved [32] and used for further applications.

2.7. *In Vitro* Studies:Cell Seeding.

Scaffolds were cut appropriately to fit into 48 well plates. These scaffolds were washed with PBS three times and then sterilized by ethylene oxide (EtO). At ~80 % confluency hUCMSCs were trypsinized and seeded on 48 well plates containing scaffold at a cell density of $1.0x10^4$ cells/mL. These seeded plates were incubated at 37 ˚C, 5% CO_2 for 1, 4 and 7 days to study cell attachment, cytotoxicity and cell proliferation activity.

Cell Attachment Study.

After 1, 4, 7 days in culture, cell-seeded scaffolds were fixed using 4% paraformaldehyde (PFA). These PFA fixed scaffolds were then analysed for cellular attachment and proliferation over scaffold surface by various methods including FESEM.

Confocal Microscopy Imaging.

Cell-seeded scaffold post 1, 4 and 7 days of incubation were fixed with 4% PFA; cells were permeabilized using permeabilization buffer. Non-specific binding sites on scaffolds were blocked using BSA and cells on scaffolds were stained using nuclear stain DAPI. Slides were mounted on mounting media and cells were imaged with a confocal microscope (Zeiss, Germany). The images were processed with Zen Software (Zeiss). Analysis with ImageJ software was performed for cell count.

MTT Cell Viability and Proliferation Assay.

MTT [3-(4, 5-dimethylthiazol-2yl)-2, 5-diphenyltetrazolium bromide**]** was prepared in DMEM (pH=7.4), filter sterilized through 0.2 µM filter in to a sterile, light-protected container. 50 µL MTT solution was added into each well with cells seeded scaffolds. After incubation of 3 h, dimethyl sulfoxide (DMSO) was added to suspend formazan crystals. The quantity of the resultant purple coloured formazan was measured at 570 nm using spectrophotometer (Hitachi) [33]. The same procedure was followed for 4th and 7th day.

2.8. Osteoblastic Differentiation.

Alizarin Red S staining for calcium.

The hUCMSCs were seeded on scaffolds for 14 and 21 days in serum-free growth media. The control was kept as tissue culture plate with osteoblastic differentiation media containing DMEM medium supplemented with ascorbic acid (50 µg/mL), β-glycerophosphate (5mM), dexamethasone ($1X10^{-7}$M), and nonessential amino acids (1%). After 14 and 21 days of culture, mineralization was analysed by staining with 2% Alizarin Red S stain (pH 4.2). After PBS wash, samples were observed for Ca^{++} minerals under an inverted phase-contrast microscope equipped with a digital camera. Quantification of osteoblast formation was performed using 10% acetic acid and 30 min of incubation. Then scaffolds were placed into a microcentrifuge tube, heated at 85 ^{0}C for 10 min then cooled and centrifuged at 10,000g for 15 min; then above solution was taken and neutralized with 10% ammonium hydroxide and the quantity of Alizarin Red S was analyzed by measuring absorbance at 405 nm [34–36].

Von Kossa staining for calcium.

Scaffolds were assessed for mineralization by using Von Kossa staining. The samples were fixed by 10% formalin and then silver nitrate ($AgNO_3$, 5%) solution was used to stain samples at room temperature for 60 min under UV light. The stain was removed and samples were visualized under an inverted phase-contrast microscope.

2.9. Statistical analysis.

Statistical analysis of all data was performed using Origin Pro 8.5 software. Statistical data was presented as Mean± standard deviation. Statistical significance was evaluated using student's t-test. (*P≤ 0.05 *; P≤ 0.005 **)*

3. RESULTS

Brown coloured callus was observed after 4 weeks of culture [37,38]. The purified form of CQ callus extract showed the presence of Phytosterol which is confirmed by Salkowski test (supporting information: Figure S2) [25, 27]. Phytosterols are osteoinductive in nature [27] and promote bone regeneration [24]. These phytosterols stimulated increased expression of osteopontin and increased uptake of minerals such as calcium, sulphur by osteoblasts in fracture healing [24]. Thus the addition of CQ callus extract in scaffold increase the potential of the scaffold in bone tissue engineering.

3.1. Preparation and Characterization of Scaffolds.

Morphological analysis.

FESEM analysis of electrospun PCL scaffolds and layer-by-layer modified scaffolds (Figure 1) showed electrospun PCL scaffolds with smooth fiber structures while layer-by- layer modified scaffolds coated with GP and CQ had rough fiber structures. Fibre diameter (Table 1) was increased in PCL-GP and compared with PCL scaffolds. Fibre diameter was significantly increased in the PCL-GP-CQ scaffolds. GP layers on PCL-GP and PCL-GP-CQ were randomly distributed throughout PCL scaffold. Fibre diameter was significantly increased with deposition of GP, and CQ in the respective scaffolds. Higher fiber diameter also aided in migration of the cells and in cell penetration [39,40]. The enhanced rough surface increases potential of protein adhesion, cell adhesion, and cell proliferation [27].

Surface properties of PCL and surface modified PCL scaffolds were analysed by atomic force microscopy (AFM) using tapping mode (supporting information). Root mean square roughness (RMS) values were PCL (146 ± 10 nm), PCL-GP (270±10 nm) and PCL-GP-CQ (278±11 nm)..The modified PCL-GP and PCL-GP-CQ scaffolds showed higher roughness as compared to PCL scaffolds.

Similarlly,the PLA films showed improved roughness and mountain-like topography after coating with polyethyleneimine-GP as compared to uncoated PLA films [15]. GP films on Si/SiO_2 showed nanoripples with high density [41]. A rough surface is beneficial in cell attachment and proliferation. Surface roughness affects the adsorption of fibronectin and albumin *in vitro* [42]. Surface roughness promotes cell attachment, adhesion, osteoblast proliferation and differentiation. It also promotes matrix synthesis and local factor production [43]. Surface roughness has a positive effect on bioactivity, water uptake and cytocompatibility of composites [44].

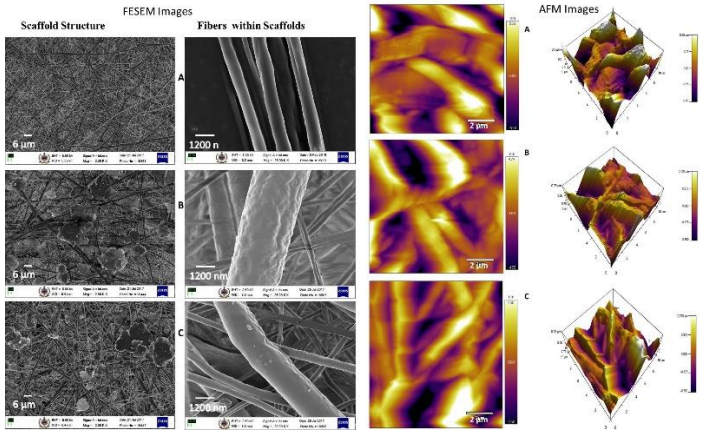

Figure 1. Field emission scanning electron microscope (FESEM) images and Atomic force microscopy (AFM) images. A: PCL; B: PCL-GP; C: PCL-GP-CQ.

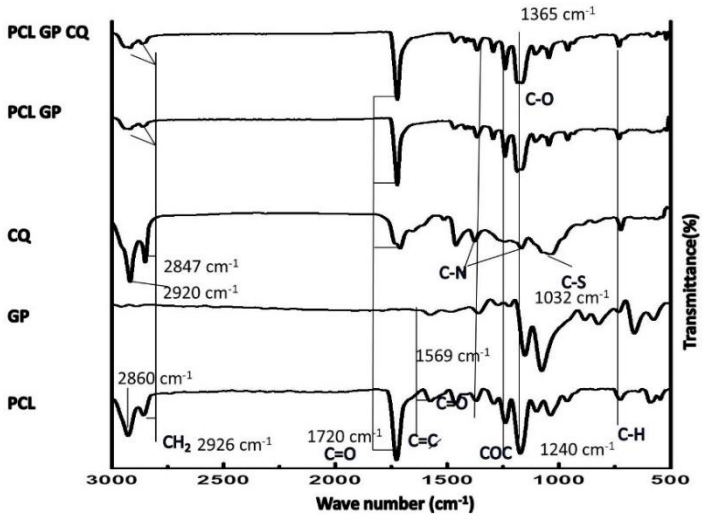

Figure 2. Fourier Transform Infra-Red spectroscopy (FTIR) spectra of the scaffolds.

Physical analysis.

FTIR spectra (Figure 2) revealed the presence of PCL, GP and CQ in respective scaffolds. Distinctive absorption peaks of asymmetric CH_2 stretching at 2926 cm^{-1} and symmetric CH_2 stretching at 2860 cm^{-1}, C=O/carbonyl stretching at 1720 cm^{-1}, C-O and C-C stretching at 1293 cm^{-1}, asymmetric C-O-C stretching at 1240 cm^{-1} were observed for PCL. C-C stretching at 1576 cm^{-1}, C-OH stretching at 1365 cm^{-1}, alkoxy C-O stretching at 1150 cm^{-1} and 1069 cm^{-1} observed for GP. Alkane asymmetric C-H stretching at 2920 cm^{-1}, alkane symmetric C-H stretching at 2847 cm^{-1}, C=O stretching at 1708 cm^{-1} and 1459 cm^{-1}, alkane C-H bending at 1377 cm^{-1} and 1163 cm^{-1}, C-N stretching at 1150 cm^{-1} -1000 cm^{-1}, C=S stretching at 1032 cm^{-1} were observed for CQ. FTIR spectra (Figure 2) confirmed the interaction of PCL with GP and CQ in respective scaffolds. In composite scaffolds, there were many overlapping peaks observed between PCL, GP and CQ, therefore they were not clearly differentiated. However, integrating and/or broadening of peaks confirmed the presence of these multiple components. The prominent peak of 1569 cm^{-1} and small peaks of GP between 2000 cm^{-1} to 2500 cm^{-1} were reduced whereas 1365 cm^{-1} peaks were broadened in PCL-GP and PCL-GP-CQ scaffolds. Similar kind of results was obtained elsewhere [27,29].

Wetting properties.

The water contact angles of PCL, layer-by-layer modified PCL-GP, PCL-GP-CQ are shown in Table 1. PCL scaffolds were hydrophobic while layer-by-layer modified scaffolds PCL-GP, and PCL-GP-CQ were hydrophilic in nature. PCL-GP-CQ scaffolds showed the lowest water contact angle and the highest hydrophilicity. Incorporation of layer by layer GP, and CQ into their respective scaffolds increased the hydrophilicity of scaffolds. This could be due to CQ having hydrophilic carboxylic and hydroxyl functional groups and their interaction with PCL [30]. Also, carbon atoms present at the edge of the graphene have special chemical reactivity to react with other materials [16]. The hydrophilicity of PLLA [29] was increased on the addition of CQ crude extract. The contact angle of PCL decreased from 133 to 37 with the addition of CQ [27].

Hydrophilic surface provides better cell attachment, spreading and proliferation of cells than hydrophobic surfaces. This hydrophilic surface allows the absorption of fibronectin which is important in osteoblast adhesion *in vitro* [43].

Mechanical Properties.

Tensile strength and Yield strength of scaffolds are shown (Table 1). Both Tensile strength and Yield strength of scaffolds were enhanced with the addition of GP and CQ into PCL scaffolds. PCL-GP-CQ scaffolds showed the highest Tensile strength and Yield strength as compared to other scaffolds.

All the modified scaffolds PCL-GP, PCL-GP-CQ showed increased Tensile strength and Yield strength as compared to PCL alone (Table 1). Tensile strength and Young's modulus of PLLA increased with the addition of CQ [29]. Tensile strength of PCL nanofibers also improved from 0.79 MPa to 2.92 MPa with the addition of CQ [27]. The scaffolds with superior mechanical strength favour cell-based bone regeneration through an endochondral ossification [45]. If the scaffolds possesses superior mechanical properties then they keep their original structure after *in vivo* implantation in load-bearing tissues such as bones [12,46]. Therefore, the mechanical properties of implanted scaffolds should be comparable with the native tissue [47,48].

3.2. Isolation and Culture of HUCMSCs.

hUCMSCs were successfully isolated from human umbilical cord Wharton's Jelly and further passaged in DMEM-HF12 medium at 37ºC, and 5% CO_2. These hUCMSCs were then used for further studies.

3.3. *In Vitro* Studies.

Cell Adhesion study.

The cells attached to PCL, PCL-GP, and PCL-GP-CQ scaffolds after 24h of culture. Morphology of these cells was fibroidal in nature. The filopodia of the cells were attached to the surface of the scaffold. The rough surface and hydrophilic nature of scaffolds contributed to better attachment and spreading of cells on

surfaces. hUCMSCs were well spread and attached to PCL-GP-CQ scaffolds (Figure 3). The obtained results were similar to those obtained by other researchers [25]. Human osteosarcoma cells (HOS) cells adhered and spread showing flat morphologies on (PBA)-PCL blended with HA scaffolds [9]. The human foetal osteoblast cells (hFOB) cells showed cuboidal osteoblast-like morphology with filopodia formation and bridging each other with the help of the extracellular matrix. Besides, the formation of mineral particles on cell surfaces was observed after 10 and 15 days of culture [27].

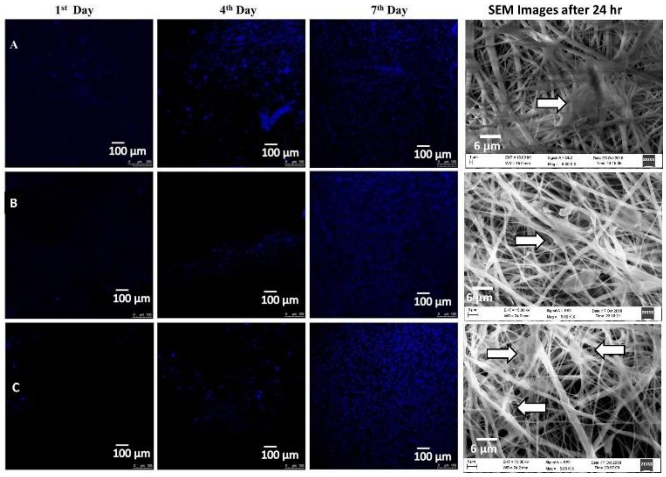

Figure 3. Confocal Microscopy Imaging from 1st day to 7th day of culture and FESEM images of cell attachment with Scaffolds after 24 hr. A: PCL; B: PCL-GP; C: PCL-GP-CQ.

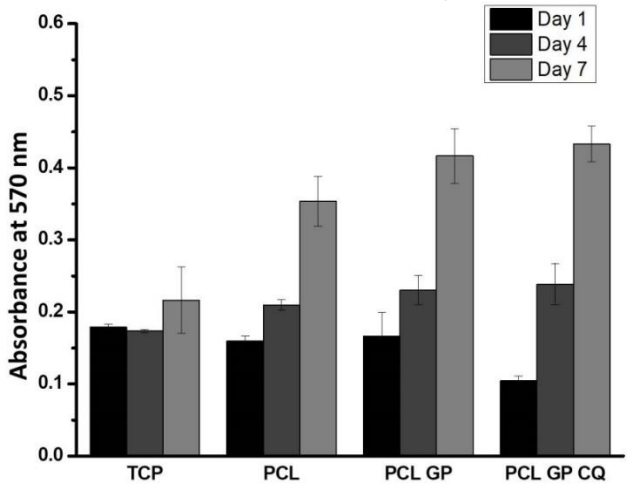

Figure 4. The cell viability and proliferation of hUCMSCs on the scaffolds for 1, 4, and 7 days of the culture studied with MTT assay (**p< 0.01).

Confocal Microscopy Imaging.

Cell-seeded scaffolds that were incubated for 1, 4 and 7 days were also stained with DAPI for nuclear visualization shown in Figure 4. These cells were in a progressive manner from 1st day to 7th day of culture. Z stack images showed cell attachment and cell movement deep into scaffold and not just on the surface. Cell count obtained with ImageJ software showed no. of cells on 1st, 4th and 7th day as 884, 2683, and 2773 on PCL; 78, 232, 2435 on PCL-GP; 76, 323, 2615 on PCL-GP-CQ respectively. All these modified scaffolds showed the highest cell proliferation on 7th day as compared to PCL scaffolds with PCL-GP-CQ scaffold exhibiting the highest cell proliferation amongst the lot.

Similar results were found in other GP containing scaffolds. The GP films showed the progressive proliferation of MSCs from day 1 to day 7 compared to PDMS (polydimethylsiloxane) or Si/SiO_2 [49]. HOS cells also showed adherence and high density on (PBA)-PCL blended with HA scaffolds via nuclei staining [9]. It showed good proliferation and penetration of cells on these scaffolds. It again showed the resemblance in terms of cell attachment on scaffolds. Rough surface and hydrophilic nature of scaffolds contributed to the proliferation of cells. The higher proliferation was due to hydrophilic and rough surfaces of scaffolds, which enhances the cellular attachement. These rough surfaces allow absorption of fibronectin which is important in osteoblast adhesion *in vitro* [42,43] and promotes cell attachment on the surfaces of composites, osteoblast proliferation, and differentiation. These hydrophilic and rough surfaces also have a positive effect on bioactivity, water uptake and cytocompatibility of composites [44].

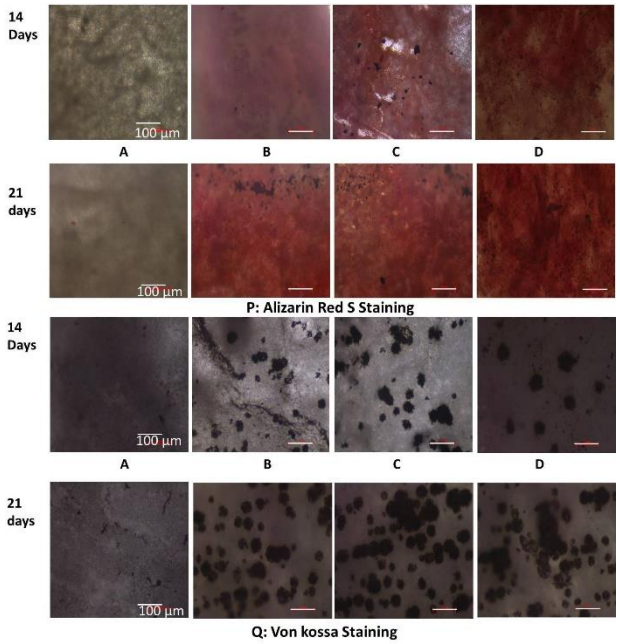

Figure 5. Alizarin Red S staining and Von Kossa staining of Layer by layer scaffolds after 14 days and 21 days of differentiation of HUCMSCs. A: PCL; B: PCL-GP; C: PCL-GP-CQ; (A to C: without Osteoblastic differentiation medium); D: Tissue culture plate with Osteoblastic differentiation medium.

MTT Cell Proliferation Assay.

The proliferation of hUCMSCs on different scaffolds was evaluated by MTT assay at a point of time on 1st, 4th, and 7th day. From Figure 4, it was evident that the proliferation of cells, as determined by the absorbance, increases from day 1 to day 7 for all scaffolds. This showed the proficiency of all scaffolds to support the proliferation of hUCMSCs. Cell proliferation on all scaffolds was found to be higher as compared to tissue culture plate and PCL from day 4th to day 7th. Cell proliferation on PCL-GP-CQ was higher as compared to other scaffolds on day 7th.

These results are comparable withthe PLAgraphene oxideand PLAgraphene nano-platelets. There was significantly greater proliferation of MG 63 celsl on GO and GNP containing PLA scaffolds [50]. HOS cells showed good biocompatibility on Poly(1,4-butylene adipate-co-polycaprolactam) (PBA)-PCL blended with HA [9]. There was comparable growth of cells on graphene-coated substrates like that of a glass slide or Si/SiO_2 [41]. PCL-CQ scaffolds showed better growth and proliferation of hFOB compared to PCL alone [27]. Cell culture experiments

demonstrated improved biocompatibility of PCL-GP, PCL-GP-CQ scaffolds as compared to PCL alone (Figure 5). The improved biocompatibilities of scaffolds were due to improved hydrophilic and rough surfaces. GP presence on the surface of scaffold improved hydrophilicity which is then required for cell adhesion and protein adsorption [25]. Vitronectin and fibronectin protein adhesion were increased in hydrophilic surfaces [50].

3.4. Osteoblastic Differentiation.

Alizarin Red S staining for calcium.

Alizarin Red S staining was used to assess calcium deposits in differentiated cells. It could be confirmed with a formation of red-orange complex.

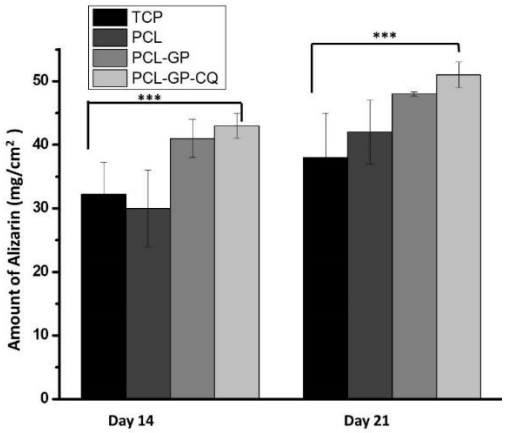

Figure 6. Alizarin Red S staining quantification of Layer by layer scaffolds after 14 days and 21 days of differentiation of hUCMSCs (*p< 0.05).

Differentiation of hUCMSCs into osteoblasts was observed from 14 days onwards. There was mineralization on PCL-GP, PCL-GP-CQ scaffolds after 14 days of culture. There was higher mineralization on PCL-GP-CQ scaffolds on the 21st day as compared to 14th day. The maximum differentiation of hUCMSCs into osteoblasts was confirmed after 21 days of culture on modified scaffolds of PCL-GP-CQ. These results indicate that the synergistic effect of GP and CQ extract could enhance the expression of osteogenic differentiation markers and can stimulate calcium deposition (Figure 5 and Figure 6). hUCMSCs differentiated on scaffolds (Figure 5. A to C) without an osteogenic medium was comparable with the control tissue culture plate (Figure 5. D) containing an osteogenic medium. Least mineralization was observed on PCL scaffolds without an osteogenic medium. These results suggest that these scaffolds have great potential for osteogenic differentiation of hUCMSCs.

There was increased activity on PCL-GP-CQ scaffolds as compared to PCL-GP and PCL scaffolds on 21 days of differentiation. It may be due to the secretion of osteocalcin by differentiated osteoblasts. Osteocalcin plays an important role in bone metabolic activities and bone-building [27]. It shows PCL-GP-CQ scaffolds as a potential bone regenerative scaffold. PLLA-CQ scaffolds also showed mineralization with simulated body fluid (SBF) after 14 days of incubation with Alizarin Red S staining [29]. The human foetal osteoblast cells also showed a higher mineralization on CQ containing scaffolds on the 15th day of culture [27]. The graphene demonstrated as an substitute to BMP-2 (Bone morphogenic growth factor-2) as it showed the similar differentiation ofhMSCs into osteoblastic cells, with a significant amount of osteocalcin secretion on the 15th day as that of BMP-2 in the presence of osteogenic media. Also, graphene supported differentiation of MSCs into osteoblasts by mineralization on 12th day in the presence of osteogenic media [41].

Von Kossa staining for calcium.

Von Kossa staining was used to evaluate secreted mineralization in differentiated cells (Figure 5). The formation of black precipitates confirmed positive Von Kossa staining. The black precipitates were observed from 14 days onwards and were maximum and broad after 21 days of culture on modified scaffolds of PCL-GP-CQ as compared to other scaffolds. hUCMSCs differentiated on the scaffolds (Figure 5. A to C) in the absence of osteogenic medium was comparable with the control tissue culture plate (Figure 5. D) containing osteogenic medium. Least mineralization was seen on PCL scaffolds without an osteogenic medium. Similar results as that of Alizarin Red S staining confirmed differentiation of hUCMSCs into osteoblasts. The osteogenic differentiation of MSCs was shown in the presence of serum and human plasma after 28 days of culture in osteogenic media [51]. There was positive Von kossa staining for MSCs cultured on biphasic calcium phosphate, calcium phosphate with conditioned medium and growth factors after 21 days [52].

Von kossa staining was used to evaluate osteoblastic differentiation of MSCs through mineralization. After 24 days of culture of MSCs into osteoblastic induction medium, there was mineralization from 14 days onwards in an increasing manner, as confirmed by Von kossa staining[53]. Foetal rat calvariae (FRC) cells cultured on osteoblastic medium showed mineralization or bone nodules formation on day 14, as confirmed by Von kossa staining [54]. BMPs were assessed for osteoinduction of MSCs for 21 days of culture. There was significant mineralization and bone nodules formation when MSCs cultured with a combination of BMP-2+BMP-6+ BMP-9 confirmed by Von kossa staining[55].

Table 1. Properties of scaffolds like fiber diameter, contact angle and mechanical properties were mentioned in the table.

Sr.No	Type of Scaffolds	Fibre Diameter (nm) (Mean ±SD)	Contact angle (Mean ±SD)	Nature of Scaffolds	Tensile strength (MPa) (Mean ±SD)	Yield strength (MPa) (Mean ±SD)
1	PCL	226.37±16.92	126.5±0.28	Hydrophobic	0.85±0.11	0.46±0.01
2	PCL-GP	1029.5±183.51	77.4±0.34	Hydrophillic	0.86±0.01	0.49±0.01
3	PCL-GP-CQ	1374.66±224.25	67.7±0.4	Hydrophillic	2.16±0.01	0.95±0.01

4. CONCLUSIONS

The prepared PCL-GP-CQ scaffolds are novel, herbal, and cell compatible with an osteoinductive nature. Their porous, rough, and hydrophilic nature, along with mechanically stable character helped hUCMSCs to adhere, spread, proliferate and spontaneously differentiate into osteoblast-like cells. The synergistic effect of GP and CQ in PCL-GP-CQ scaffold enhanced the roughness, mechanical properties, and wettability of scaffolds. Mainly GP and CQ callus extract provided osteoinductive properties to scaffold

that helped hUCMSCs to spontaneously differentiate into osteoblast without any osteogenic media or growth factors or added external stimuli. This property helps the scaffold to accelerate *in vivo* bone formation upon transplantation, thus saving *in vitro* differentiation time before transplantation. Also, the novel scaffold causes early remodeling of bone even in critical size defect which otherwise difficult to heal. Thus, the novel PCL-GP-CQ scaffold prepared using layer-by-layer method revealed the high potential for *in vivo* bone tissue engineering and bone regeneration.

5. REFERENCES

1. Venkatesan, J.; Bhatnagar, I.; Kim, S.K. Chitosan-alginate biocomposite containing fucoidan for bone tissue engineering. *Mar Drugs* **2014**, *12*, 300-316, https://doi.org/10.3390/md12010300.
2. Kashte, S.; Jaiswal, A.K.; Kadam, S. Artificial Bone via Bone Tissue Engineering: Current Scenario and Challenges. *Tissue Engineering and Regenerative Medicine* **2017**, *14*, 1-14, https://doi.org/10.1007/s13770-016-0001-6.
3. Alves, A.; Duarte, A.R.C.; Mano, J.F.; Sousa, R.A.; Reis, R.L. PDLLA enriched with ulvan particles as a novel 3D porous scaffold targeted for bone engineering. *The Journal of Supercritical Fluids* **2012**, *65*, 32-38, https://doi.org/10.1016/j.supflu.2012.02.023.
4. Rajzer, I.; Menaszek, E.; Kwiatkowski, R.; Chrzanowski, W. Bioactive nanocomposite PLDL/nano-hydroxyapatite electrospun membranes for bone tissue engineering. *Journal of Materials Science: Materials in Medicine* **2014**, *25*, 1239-1247, https://doi.org/10.1007/s10856-014-5149-9.
5. Liu, X.; Ma, P.X. Polymeric Scaffolds for Bone Tissue Engineering. *Annals of Biomedical Engineering* **2004**, *32*, 477-486.
6. Qian, J.; Xu, W.; Yong, X.; Jin, X.; Zhang, W. Fabrication and in vitro biocompatibility of biomorphic PLGA/nHA composite scaffolds for bone tissue engineering. *Materials Science and Engineering: C* **2014**, *36*, 95-101, https://doi.org/10.1016/j.msec.2013.11.047.
7. Chuenjitkuntaworn, B.; Osathanon, T.; Nowwarote, N.; Supaphol, P.; Pavasant, P. The efficacy of polycaprolactone/hydroxyapatite scaffold in combination with mesenchymal stem cells for bone tissue engineering. *Journal of Biomedical Materials Research Part A* **2016**, *104*, 264-271, https://doi.org/10.1002/jbm.a.35558.
8. Ren, K.; Wang, Y.; Sun, T.; Yue, W.; Zhang, H. Electrospun PCL/gelatin composite nanofiber structures for effective guided bone regeneration membranes. *Materials Science and Engineering: C* **2017**, *78*, 324-332, https://doi.org/10.1016/j.msec.2017.04.084.
9. Chakrapani, V.Y.; Kumar, T.S.S.; Raj, D.K.; Kumary, T.V. Electrospun Cytocompatible Polycaprolactone Blend Composite with Enhanced Wettability for Bone Tissue Engineering. *Journal of Nanoscience and Nanotechnology* **2017**, *17*, 2320-2328, https://doi.org/10.1166/jnn.2017.13713.
10. Son, Y.J.; Kim, H.S.; Yoo, H.S. Layer-by-layer surface decoration of electrospun nanofibrous meshes for air–liquid interface cultivation of epidermal cells. *RSC Advances* **2016**, *6*, 114061-114068, https://doi.org/10.1039/C6RA23287F.
11. Gallagher, W.M.; Lynch, I.; Allen, L.T.; Miller, I.; Penney, S.C.; O'Connor, D.P.; Pennington, S.; Keenan, A.K.; Dawson, K.A. Molecular basis of cell–biomaterial interaction: Insights gained from transcriptomic and proteomic studies. *Biomaterials* **2006**, *27*, 5871-5882, https://doi.org/10.1016/J.BIOMATERIALS.2006.07.040.
12. Yang, S.; Leong, K.-F.; Du, Z.; Chua, C.-K. The Design of Scaffolds for Use in Tissue Engineering. Part I. Traditional Factors. *Tissue Engineering* **2001**, *7*, 679-689, https://doi.org/10.1089/107632701753337645.
13. Chen, W.; McCarthy, T.J. Layer-by-Layer Deposition: A Tool for Polymer Surface Modification. *Macromolecules* **1997**, *30*, 78-86, https://doi.org/10.1021/ma961096d.
14. Li, Y.; Choi, M.-C.; Jeong, K.-M.; Jeong, J.H.; Lee, H.-G.; Kim, G.H.; Ha, C.S. Layer-by-layer assembly of graphene on polyimide films via thermal imidization and synchronous reduction of graphene oxide. *Macromolecular Research* **2017**, *25*, 496-499, https://doi.org/10.1007/s13233-017-5093-x.
15. He, X.; Wu, L.-l.; Wang, J.-j.; Zhang, T.; Sun, H.; Shuai, N. Layer-by-layer assembly deposition of graphene oxide on poly(lactic acid) films to improve the barrier properties. *High Performance Polymers* **2015**, *27*, 318-325, https://doi.org/10.1177/0954008314545978.
16. Agharkar, M.; Kochrekar, S.; Hidouri, S.; Azeez, M.A. Trends in green reduction of graphene oxides, issues and challenges: A review. *Materials Research Bulletin* **2014**, *59*, 323-328, https://doi.org/10.1016/j.materresbull.2014.07.051.
17. [Zhang, Q.; Li, K.; Yan, J.; Wang, Z.; Wu, Q.; Bi, L.; Yang, M.; Han, Y. Graphene coating on the surface of CoCrMo alloy enhances the adhesion and proliferation of bone marrow mesenchymal stem cells. *Biochemical and Biophysical Research Communications* **2018**, *497*, 1011-1017, https://doi.org/10.1016/j.bbrc.2018.02.152.
18. Qiu, J.; Guo, J.; Geng, H.; Qian, W.; Liu, X. Three-dimensional porous graphene nanosheets synthesized on the titanium surface for osteogenic differentiation of rat bone mesenchymal stem cells. *Carbon* **2017**, *125*, 227-235, https://doi.org/10.1016/j.carbon.2017.09.064.
19. Jaidev, L.R.; Kumar, S.; Chatterjee, K. Multi-biofunctional polymer graphene composite for bone tissue regeneration that elutes copper ions to impart angiogenic, osteogenic and bactericidal properties. *Colloids and Surfaces B: Biointerfaces* **2017**, *159*, 293-302, https://doi.org/10.1016/j.colsurfb.2017.07.083.
20. Mishra, G.; Nagori, B.P. Pharmacological and therapeutic activity of Cissus quadrangularis: An overview. *International Journal of PharmTech Research* **2010**, *2*, 1298-1310.
21. Deka, D.; Lahon, L.; Saikia, J.; Mukit, A. Effect of Cissus quadrangularis in accelerating healing process of experimentally fractured radius-ulna of dog: A preliminary study. *Indian Journal of Pharmacology* **1994**, *26*, 44–45.
22. Rao, M.; Potu, B.; Swamy, N.; N, G. Cissus quadrangularis plant extract enhances the development of cortical bone and trabeculae in the fetal femur. *Pharmacologyonline* **2007**, *3*. 190–202.
23. Potu, B.K.; Rao, M.S.; Kutty, N.G.; Bhat, K.M.R.; Chamallamudi, M.R.; Nayak, S.R. Petroleum ether extract of Cissus quadrangularis (LINN) stimulates the growth of fetal bone during intra uterine developmental period: a morphometric analysis. *Clinics* **2008**, *63*, 815-820, https://doi.org/10.1590/S1807-59322008000600018.
24. Singhal, A.; Hadi, R.; Chaturvedi, A.; Sharma, I.; Misra, S.; Husain, N. Vascular endothelial growth factor expression in oral cancer and its role as a predictive marker: A prospective study. *National Journal of Maxillofacial Surgery* **2013**, *4*, 52-56, https://doi.org/10.4103/0975-5950.117884.
25. Kashte, S.; Arbade, G.; Sharma, R.K.; Kadam, S. Herbally Painted Biofunctional Scaffolds with Improved Osteoinductivity

for Bone Tissue Engineering. *Journal of Biomimetics, Biomaterials and Biomedical Engineering* **2019**, *41*, 49-68, https://doi.org/10.4028/www.scientific.net/jbbbe.41.49.
26. Kashte, S.; Sharma, R.K.; Kadam, S. Layer-by-layer decorated herbal cell compatible scaffolds for bone tissue engineering: A synergistic effect of graphene oxide and Cissus quadrangularis. *Journal of Bioactive and Compatible Polymers* **2020**, *35*, 57-73, https://doi.org/10.1177/0883911519894667 .
27. Suganya, S.; Venugopal, J.; Ramakrishna, S.; Lakshmi, B.S.; Giri Dev, V.R. Herbally derived polymeric nanofibrous scaffolds for bone tissue regeneration. *Journal of Applied Polymer Science* **2014**, *131*, 1–11, https://doi.org/10.1002/app.39835.
28. Stankovich, S.; Dikin, D.A.; Piner, R.D.; Kohlhaas, K.A.; Kleinhammes, A.; Jia, Y.; Wu, Y.; Nguyen, S.T.; Ruoff, R.S. Synthesis of graphene-based nanosheets via chemical reduction of exfoliated graphite oxide. *Carbon* **2007**, *45*, 1558-1565, https://doi.org/10.1016/j.carbon.2007.02.034.
29. Parvathi, K.; Krishnan, A.G.; Anitha, A.; Jayakumar, R.; Nair, M.B. Poly(L-lactic acid) nanofibers containing Cissus quadrangularis induced osteogenic differentiation in vitro. *International Journal of Biological Macromolecules* **2018**, *110*, 514-521, https://doi.org/10.1016/j.ijbiomac.2017.11.094.
30. Zhou, T.; Li, G.; Lin, S.; Tian, T.; Ma, Q.; Zhang, Q.; Shi, S.; Xue, C.; Ma, W.; Cai, X.; Lin, Y. Electrospun Poly(3-hydroxybutyrate-co-4-hydroxybutyrate)/Graphene Oxide Scaffold: Enhanced Properties and Promoted in Vivo Bone Repair in Rats. *ACS Applied Materials & Interfaces* **2017**, *9*, 42589-42600, https://doi.org/10.1021/acsami.7b14267.
31. Kadam, S.S.; Sudhakar, M.; Nair, P.D.; Bhonde, R.R. Reversal of experimental diabetes in mice by transplantation of neo-islets generated from human amnion-derived mesenchymal stromal cells using immuno-isolatory macrocapsules. *Cytotherapy* **2010**, *12*, 982-991, https://doi.org/10.3109/14653249.2010.509546.
32. Kadam, S.S.; Bhonde, R.R. Islet neogenesis from the constitutively nestin expressing human umbilical cord matrix derived mesenchymal stem cells. *Islets* **2010**, *2*, 112-120, https://doi.org/10.4161/isl.2.2.11280.
33. Jaiswal, A.K.; Kadam, S.S.; Soni, V.P.; Bellare, J.R. Improved functionalization of electrospun PLLA/gelatin scaffold by alternate soaking method for bone tissue engineering. *Applied Surface Science* **2013**, *268*, 477-488, https://doi.org/10.1016/j.apsusc.2012.12.152.
34. Thadavirul, N.; Pavasant, P.; Supaphol, P. Fabrication and Evaluation of Polycaprolactone–Poly(hydroxybutyrate) or Poly(3-Hydroxybutyrate-co-3-Hydroxyvalerate) Dual-Leached Porous Scaffolds for Bone Tissue Engineering Applications. *Macromolecular Materials and Engineering* **2017**, *302*, https://doi.org/10.1002/mame.201600289.
35. Tsai, K.-Y.; Lin, H.-Y.; Chen, Y.-W.; Lin, C.-Y.; Hsu, T.-T.; Kao, C.-T. Laser Sintered Magnesium-Calcium Silicate/Poly-ε-Caprolactone Scaffold for Bone Tissue Engineering. *Materials* **2017**, *10*, 65–72, https://doi.org/10.3390/ma10010065.
36. Chhabra, H.; Kumbhar, J.; Rajwade, J.; Jadhav, S.; Paknikar, K.; Jadhav, S.; Bellare, J.R. Three-dimensional scaffold of gelatin–poly(methyl vinyl ether-alt-maleic anhydride) for regenerative medicine: Proliferation and differentiation of mesenchymal stem cells. *Journal of Bioactive and Compatible Polymers* **2016**, *31*, 273-290, https://doi.org/10.1177/0883911515617491.
37. Garg, P.; Malik, C.P. Multiple shoot formation and efficient root induction in Cissus quadrangularis *Int. J. Pharm. Clin. Res.* **2012,** *4*, 4–10.
38. Mehta, P.S.R.; Teware, K. In vitro Callus Induction from Stem Explants of Cissus quadrangularis L. (Hadjod). *Int. J. Ayurvedic Herb. Med.* **2012,** *2*, 229–233.
39. Sisson, K.; Zhang, C.; Farach-Carson, M.C.; Chase, D.B.; Rabolt, J.F. Fiber diameters control osteoblastic cell migration and differentiation in electrospun gelatin. *Journal of Biomedical Materials Research Part A* **2010**, *94A*, 1312-1320, https://doi.org/10.1002/jbm.a.32756.
40. Noriega, S.E.; Noriega, S.E.; Hasanova, G.I.; Schneider, M.J.; Larsen, G.F.; Subramanian, A. Effect of Fiber Diameter on the Spreading, Proliferation and Differentiation of Chondrocytes on Electrospun Chitosan Matrices. *Cells Tissues Organs* **2012**, *195*, 207-221, https://doi.org/10.1159/000325144.
41. Nayak, T.R.; Andersen, H.; Makam, V.S.; Khaw, C.; Bae, S.; Xu, X.; Ee, P.-L.R.; Ahn, J.-H.; Hong, B.H.; Pastorin, G.; Özyilmaz, B. Graphene for Controlled and Accelerated Osteogenic Differentiation of Human Mesenchymal Stem Cells. *ACS Nano* **2011**, *5*, 4670-4678, https://doi.org/10.1021/nn200500h.
42. Deligianni, D.D.; Katsala, N.; Ladas, S.; Sotiropoulou, D.; Amedee, J.; Missirlis, Y.F. Effect of surface roughness of the titanium alloy Ti–6Al–4V on human bone marrow cell response and on protein adsorption. *Biomaterials* **2001**, *22*, 1241-1251, https://doi.org/10.1016/S0142-9612(00)00274-X.
43. Yang, M.; Zhu, S.; Chen, Y.; Chang, Z.; Chen, G.; Gong, Y.; Zhao, N.; Zhang, X. Studies on bone marrow stromal cells affinity of poly (3-hydroxybutyrate-co-3-hydroxyhexanoate). *Biomaterials* **2004**, *25*, 1365-1373, https://doi.org/10.1016/J.BIOMATERIALS.2003.08.018.
44. Misra, S.K.; Ansari, T.; Mohn, D.; Valappil, S.P.; Brunner, T.J.; Stark, W.J.; Roy, I.; Knowles, J.C.; Sibbons, P.D.; Jones, E.V.; Boccaccini, A.R.; Salih, V. Effect of nanoparticulate bioactive glass particles on bioactivity and cytocompatibility of poly(3-hydroxybutyrate) composites. *Journal of The Royal Society Interface* **2010**, *7*, 453-465, https://doi.org/10.1098/rsif.2009.0255.
45. Sun, H.; Zhu, F.; Hu, Q.; Krebsbach, P.H. Controlling stem cell-mediated bone regeneration through tailored mechanical properties of collagen scaffolds. *Biomaterials* **2014**, *35*, 1176-1184, https://doi.org/10.1016/j.biomaterials.2013.10.054.
46. Lin, C.Y.; Kikuchi, N.; Hollister, S.J. A novel method for biomaterial scaffold internal architecture design to match bone elastic properties with desired porosity. *Journal of Biomechanics* **2004**, *37*, 623-636, https://doi.org/10.1016/J.JBIOMECH.2003.09.029.
47. Arafat, M.T.; Gibson, I.; Li, X. State of the art and future direction of additive manufactured scaffolds-based bone tissue engineering. *Rapid Prototyp. J.* **2014,** *20*, 13–26, https://doi.org/10.1108/RPJ-03-2012-0023.
48. Wang, J.; Yu, X. Preparation, characterization and in vitro analysis of novel structured nanofibrous scaffolds for bone tissue engineering. *Acta Biomaterialia* **2010**, *6*, 3004-3012, https://doi.org/10.1016/j.actbio.2010.01.045.
49. Lee, W.C.; Lim, C.H.Y.X.; Shi, H.; Tang, L.A.L.; Wang, Y.; Lim, C.T.; Loh, K.P. Origin of Enhanced Stem Cell Growth and Differentiation on Graphene and Graphene Oxide. *ACS Nano* **2011**, *5*, 7334-7341, https://doi.org/10.1021/nn202190c.
50. Pinto, A.M.; Moreira, S.; Gonçalves, I.C.; Gama, F.M.; Mendes, A.M.; Magalhães, F.D. Biocompatibility of poly(lactic acid) with incorporated graphene-based materials. *Colloids and Surfaces B: Biointerfaces* **2013**, *104*, 229-238, https://doi.org/10.1016/j.colsurfb.2012.12.006.
51. Felka, T.; Schäfer, R.; De Zwart, P.; Aicher, W.K. Animal

serum-free expansion and differentiation of human mesenchymal stromal cells. *Cytotherapy* **2010**, *12*, 143-153, https://doi.org/10.3109/14653240903470647.
52. Wang, J.; Liu, D.; Guo, B.; Yang, X.; Chen, X.; Zhu, X.; Fan, Y.; Zhang, X. Role of biphasic calcium phosphate ceramic-mediated secretion of signaling molecules by macrophages in migration and osteoblastic differentiation of MSCs. *Acta Biomaterialia* **2017**, *51*, 447-460, https://doi.org/10.1016/j.actbio.2017.01.059.
53. Hung, P.S.; Kuo, Y.C.; Chen, H.G.; Chiang, H.H.K.; Lee, O.K.S. Detection of Osteogenic Differentiation by Differential Mineralized Matrix Production in Mesenchymal Stromal Cells by Raman Spectroscopy. *PLOS ONE* **2013**, *8*, 1–7, https://doi.org/10.1371/journal.pone.0065438.
54. Yamamoto, N.; Furuya, K.; Hanada, K. Progressive Development of the Osteoblast Phenotype during Differentiation of Osteoprogenitor Cells Derived from Fetal Rat Calvaria: Model for *in Vitro* Bone Formation. *Biological and Pharmaceutical Bulletin* **2002**, *25*, 509-515, https://doi.org/10.1248/bpb.25.509.
55. Açil, Y.; Ghoniem, A.-A.; Wiltfang, J.; Gierloff, M. Optimizing the osteogenic differentiation of human mesenchymal stromal cells by the synergistic action of growth factors. *Journal of Cranio-Maxillofacial Surgery* **2014**, *42*, 2002-2009, https://doi.org/10.1016/j.jcms.2014.09.006.

6. ACKNOWLEDGEMENTS

The authors would like to acknowledge University Grant Commission (UGC), Government of India, New Delhi, for a doctoral fellowship to Mr. Shivaji Kashte.

Supplementary information

Leaching Study.

The leaching of the additives (GP) from the scaffolds was investigated as per ISO-10993-12. Experiments were performed in batch mode as incubated with extractants. The 0.1 g of scaffolds per 1 ml of distilled water was incubated at 37 ^{0}C for 72 hours. The concentration of GP in the obtained extracts was determined by measuring the absorbance at 233 nm for GP using a UV-visible spectrophotometer. The standard calibration curve of GP was also plotted to calculate their respective concentrations. Ultraviolet-visible (UV-Vis) absorption spectra were recorded using a 1cm path length quartz cuvette with distilled water as the reference on a U-2001 UV/Vis Spectrophotometer (Hitachi). Depending on the binding of these substrates scaffolds were selected for further study (Figure S1).

The leaching was least in the 60 cycles followed by overnight dipped samples and then 30 cycles. This could be due to more interaction between PCL and GP in the 60 dipped cycles. In the overnight dipped samples, the deposition was not uniform. Therefore, we are choosing 60 cycles over 30 cycles and overnight dipped samples as because of more uniform deposition as well as less leaching. The leaching study is not significant as there is a very small amount of GP in the leached solution.

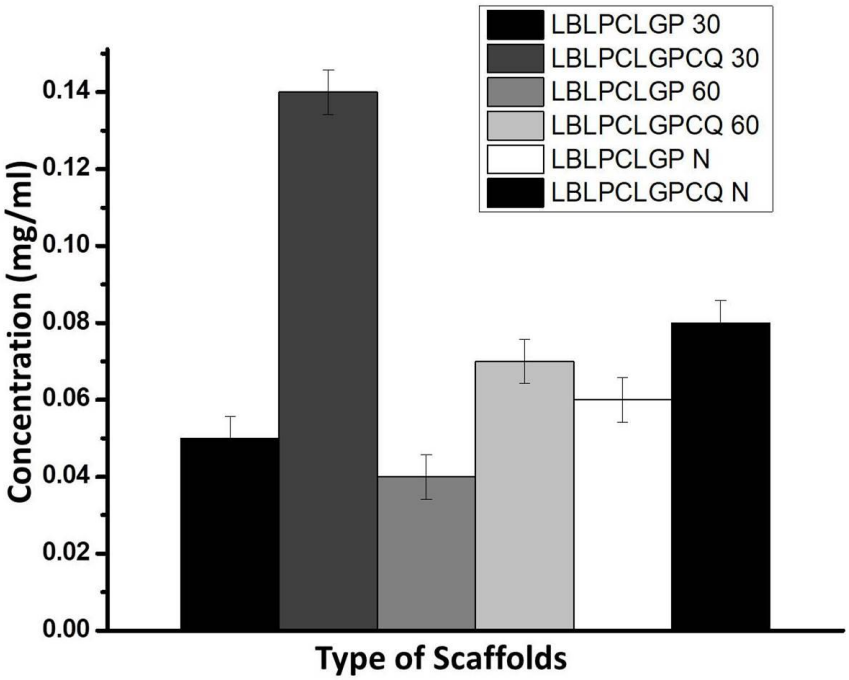

Figure S1. Leaching study of Scaffolds.

Other Supplementary Figures:

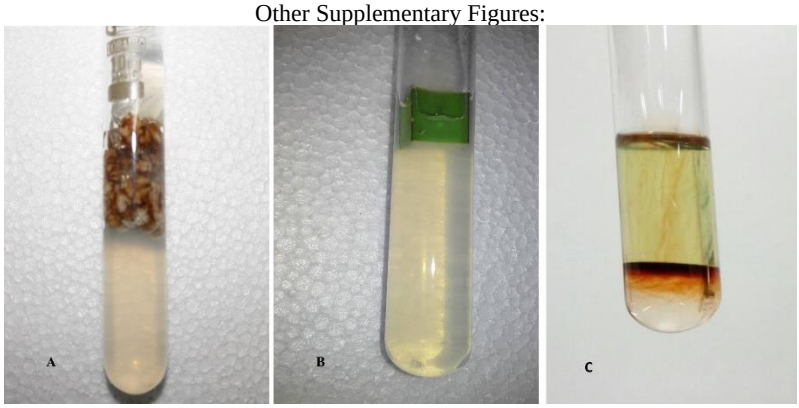

Figure S2. CQ callus culture. A: Callus formed from CQ stem explant; B: Control CQ stem explant; C: Salwoski test. The brown ring formed at the bottom of the test tube confirms the presence of phytosterols in the callus extract.